Lorenz, W. Schaffner, *Eur. J. Immunol.* **26**, 3214 (1996).
12. M. P. Kamps, L. Corcoran, J. H. LeBowitz, D. Baltimore, *Mol. Cell. Biol.* **10**, 5464 (1990).
13. I. Pfeuffer *et al.*, *J. Immunol.* **153**, 5572 (1994).
14. V. Gruart-Gouilleux, P. Engels, M. Sullivan, *Eur. J. Immunol.* **25**, 1431 (1995).
15. K. S. Ullman, J. P. Northrop, A. Admon, G. R. Crabtree, *Genes Dev.* **7**, 188 (1993).
16. Different octamer-dependent reporter constructs (wild-type and mutant versions of 4xwt.TATA and ED.TATA) were used for transient transfections of Jurkat cells (*4*). CMV lacZ was cotransfected to control for differences in transfection efficiencies. Immediately after transfection, cells were split into different dishes and induced with PMA (10 ng/ml), ionomycin (1 μg/ml), CsA (100 ng/ml), or FK 506 (1 ng/ml). Extracts for enzyme assays were prepared 18 hours after transfection.
17. Total cytoplasmic RNA (10 μg) was analyzed as described (*24*). For protein immunoblots, 100 μg of whole-cell extracts were run on 12.5% SDS-polyacrylamide gels, transferred to polyvinylidene difluoride membranes, and probed with affinity-purified antibodies to BOB.1/OBF.1. Blots were developed with the ECL-system (Amersham) (*8*). When NIH/3T3 cells were analyzed, no increased BOB.1/OBF.1 RNA or protein expression was observed after PMA and ionomycin stimulation. Anisomycin (100 μM) and FK506 (1 ng/ml) inhibited the increase of BOB.1/OBF.1 RNA and protein expression.
18. Stable transfectants of Jurkat cells were generated with the two components of the tet-regulated system (*25*).
19. BOB.1/OBF.1 was immunoprecipitated from B cell extracts or induced Jurkat T cell extracts, and precipitates were treated with calf intestinal alkaline phosphatase or λ phosphatase. Efficient dephosphorylation was confirmed by including an in vitro phosphorylated protein in some of the samples. Subsequent analysis of the dephosphorylated immunoprecipitates did not show a decrease in the 35-kD band or an increase in the 34-kD band.
20. All COOH terminally deleted and point-mutated fragments of BOB.1/OBF.1 used for GAL fusion and GST fusion experiments were generated by polymerase chain reaction (PCR) amplification followed by sequence analysis. Details on the primers used are available upon request. The different subfragments were cloned in frame into either the expression vectors containing the DNA-binding domain of the GAL4 protein (amino acids 1 to 92) (*26*) or the GST gene in the pGEX-3X (Pharmacia) vector. GST fusion proteins were expressed in bacteria and purified by glutathione sepharose chromatography.
21. W. J. Boyle, P. van der Geer, T. Hunter, *Methods Enzymol.* **201**, 110 (1991).
22. HAFTL I B cells and Jurkat T cells were labeled for 14 hours with [^{32}P]orthophosphate (1 mCi/ml) in a total of 10 ml of medium containing dialyzed fetal bovine serum. BOB.1/OBF.1 protein was immunoprecipitated from whole-cell extracts with the use of affinity-purified antibodies (*8*) and separated on 12% SDS-polyacrylamide gels. Wet gels were autoradiographed, and BOB.1/OBF.1 was excised and eluted from the gel. After cleavage with 100 ng of V8 protease (Glu-C endopeptidase, Boehringer Mannheim) for 15 hours at 30°C, phosphopeptides were separated on cellulose plates by electrophoresis at pH 1.9 followed by chromatography (*21*). Phospho–amino acid analysis was performed as described (*21*) for in vivo–labeled proteins, and only phosphoserine and phosphothreonine were identified.
23. Jurkat cells were grown in medium containing low concentrations of serum (0.5% fetal bovine serum) for 16 hours, followed by treatment with PMA (10 ng/ml), ionomycin (1 μg/ml), CsA (100 ng/ml), or FK506 (1 ng/ml) for 15 min. Cells were collected, washed three times with cold phosphate-buffered saline, and lysed in 200 μl of lysis buffer [10 mM tris (pH 7.0), 30 mM sodium pyrophosphate, 100 μM $NaVO_4$, 2 mM iodoacetic acid, 50 mM NaCl, 50 mM NaF, 5 μM $ZnCl_2$, and 1% Triton X-100]. Extracts were clarified by a 20-min spin in the Eppendorf centrifuge at 4°C. We incubated 20 μg of cell extract with 500 ng GST fusion protein in kinase buffer [20 mM tris (pH 7.5), 100 mM NaCl, 12 mM $MgCl_2$, 100 μM $NaVO_4$, and 1 mM dithiothreitol] containing 10 μCi [γ-^{32}P]ATP for 30 min at 30°C in a total volume of 40 μl. Subsequently, the fusion protein was purified by affinity chromatography using glutathione agarose beads. Proteins were dissociated from the resin by boiling in SDS sample buffer and then were subjected to 12% SDS–polyacrylamide gel electrophoresis.
24. H. König, P. Pfisterer, L. Corcoran, T. Wirth, *Genes Dev.* **9**, 1598 (1995).
25. M. Gossen and H. Bujard, *Proc. Natl. Acad. Sci. U.S.A.* **89**, 5547 (1992).
26. A. Annweiler, S. Zwilling, T. Wirth, *Nucleic Acids Res.* **22**, 4250 (1994).
27. We thank Sandoz Pharma and Fujisawa Pharma for the gift of CsA and FK506, respectively. We also thank R. Röder for typing the manuscript and S. Pfränger for preparing the figures. Supported by grants from the Deutsche Forschungsgemeinschaft to T.W. (SFB 229 and SFB 465) and P.A. (An 182/7-1) and by Boehringer Ingelheim.

6 January 1997; accepted 15 May 1997

Induction of Cell Migration by Matrix Metalloprotease–2 Cleavage of Laminin-5

Gianluigi Giannelli, Jutta Falk-Marzillier, Oronzo Schiraldi, William G. Stetler-Stevenson, Vito Quaranta*

Structural changes in the extracellular matrix are necessary for cell migration during tissue remodeling and tumor invasion. Specific cleavage of laminin-5 (Ln-5) by matrix metalloprotease–2 (MMP2) was shown to induce migration of breast epithelial cells. MMP2 cleaved the Ln-5 γ2 subunit at residue 587, exposing a putative cryptic promigratory site on Ln-5 that triggers cell motility. This altered form of Ln-5 is found in tumors and in tissues undergoing remodeling, but not in quiescent tissues. Cleavage of Ln-5 by MMP2 and the resulting activation of the Ln-5 cryptic site may provide new targets for modulation of tumor cell invasion and tissue remodeling.

Cell migration across extracellular matrix (ECM) tissue boundaries is required in many important biological processes, including tissue remodeling and tumor invasion (*1*, *2*). To overcome ECM barriers, advancing cells may focus proteases such as metalloproteases (*2*) or protease activators such as urokinase (*1*, *2*) at their leading edge, where complex proteolysis (*1*) can direct migration, preserve ECM attachment, or avoid unwanted tissue damage. The precise mechanisms by which proteases alter ECM components remain unresolved, and it is unclear whether proteases simply remove physical barriers to migration or mold ECM components into substrates suitable for migration.

We report that the matrix metalloprotease MMP2 induces the migration of breast epithelial cells by cleaving and regulating the function of a specific ECM component, Ln-5 (also known as kalinin, epiligrin, nicein, and ladsin). Ln-5 is a component of epithelial basement membranes, which also contain collagen type IV (Coll IV), laminin-1 (Ln-1), and, during tissue remodeling, fibronectin (Fn) (*3*). Cells adhere to or migrate on these ECM substrates by means of integrin receptors. For example, Ln-5 interaction with integrins is essential for the adhesion of epithelial cells to basement membranes (*4*) and promotes migration (*5*).

To test whether the effect of these basement membrane components on cell migration is protease-dependent, we studied their interaction with MMP2 (gelatinase A, 72-kD type IV collagenase), a protease that is concentrated along basement membranes at sites of tissue remodeling (*1*) and at the leading edge of invading tumors (*1*, *2*, *6*). In a transwell migration assay (*7*), normal human breast epithelial cells (HUMEC) or the nontumorigenic breast cell line MCF10 (*8*) adhered to the top side of the filter without crossing to the other side (Fig. 1A), which was coated with one or more purified ECM components (Coll IV, Ln-1, Fn, or Ln-5). Addition of MMP2 to the cells caused a dose-dependent induction of migration on Ln-5 (Fig. 1A), but not on any of the other three substrates. This result was surprising because Coll IV, Ln-1, and Fn have each been identified as an MMP2-recognized substrate (*1*) and might be expected to induce protease-dependent migration. Ln-5, on the other hand, has not been previously recognized as a target for MMP2. However, when filters were coated with Ln-5 pretreated in a solution containing different concentrations of MMP2 (Fig.

G. Giannelli, Department of Cell Biology, Scripps Research Institute, La Jolla, CA 92037, USA, and Institute of Clinica Medica II, Università degli Studi Bari, 70124 Bari, Italy.
J. Falk-Marzillier and V. Quaranta, Department of Cell Biology, Scripps Research Institute, La Jolla, CA 92037, USA.
O. Schiraldi, Institute of Clinica Medica II, Università degli Studi Bari, 70124 Bari, Italy.
W. G. Stetler-Stevenson, Laboratory of Pathology, National Cancer Institute, National Institutes of Health, Bethesda, MD 20892, USA.

*To whom correspondence should be addressed. E-mail: quaranta@scripps.edu

1B), or when Ln-5–coated filters were treated with MMP2 before cell addition (9), both HUMEC and MCF10 cells migrated. This result indicated that the promigratory effect of Ln-5 depends on interaction with MMP2.

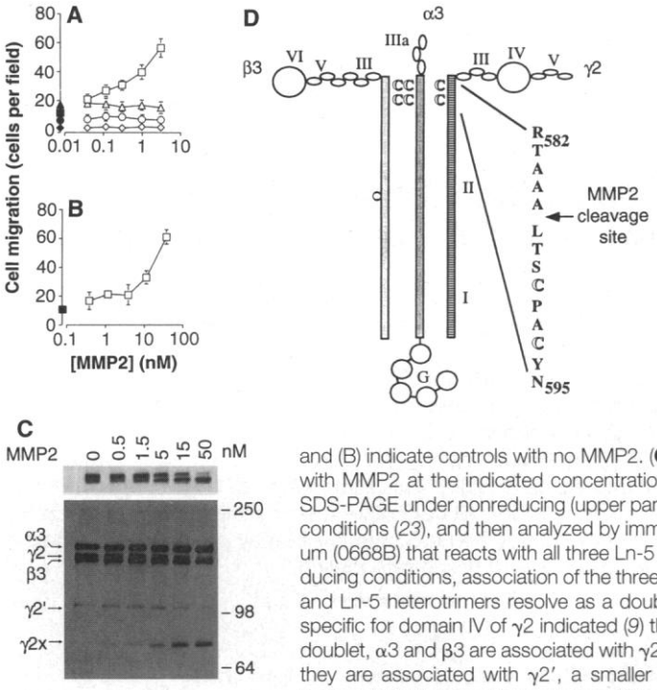

Fig. 1. Induction of cell migration by MMP2 cleavage of the Ln-5 γ2 subunit at residue 587. (**A**) Addition of activated recombinant MMP2 (*21*) to the assay medium (*22*) induces migration of HUMEC and MCF10 (*9*) cells on filters coated with Ln-5 (□), but not with Coll IV (○), Ln-1 (◇), or Fn (△). (**B**) Statistically significant migration ($P < 0.003$) occurs on filters coated with Ln-5 pretreated in solution with ≥1 nM MMP2 (□). Solid symbols in (A) and (B) indicate controls with no MMP2. (**C**) Purified Ln-5 was treated with MMP2 at the indicated concentrations, electrophoresed by 6% SDS-PAGE under nonreducing (upper panel) or reducing (lower panel) conditions (*23*), and then analyzed by immunoblotting with an antiserum (0668B) that reacts with all three Ln-5 subunits (*12*). Under nonreducing conditions, association of the three Ln-5 subunits is preserved, and Ln-5 heterotrimers resolve as a doublet. Reactivity with antisera specific for domain IV of γ2 indicated (*9*) that in the upper band of the doublet, α3 and β3 are associated with γ2, whereas in the lower band they are associated with γ2′, a smaller proteolytic derivative of γ2 lacking 413 NH_2-terminal residues (*24*). MMP2 treatment causes a dose-dependent decrease in the molecular mass of Ln-5 (~400 kD), presumably by removal of a fragment from the heterotrimers. Under reducing conditions, the three Ln-5 subunits are dissociated. The γ2 and γ2′ bands disappear proportionally to MMP2 concentration, whereas α3 and β3 are unchanged, even at higher MMP2 concentrations (500 nM) (*9*). The new band at 80 kD (γ2x) is a γ2 (and probably γ2′) digestion product, because it reacts with a γ2-specific antiserum (*9*). (**D**) Schematic representation of the MMP2 cleavage site on Ln-5, identified by microsequencing (*23*) of the γ2x protein. Cysteines are not detected by automated microsequencing and were deduced from cDNA (*23*). The G domain of Ln-5 is indicated at the bottom. Abbreviations for amino acid residues: A, Ala; C, Cys; L, Leu; N, Asn; P, Pro; R, Arg; S, Ser; T, Thr; and Y, Tyr.

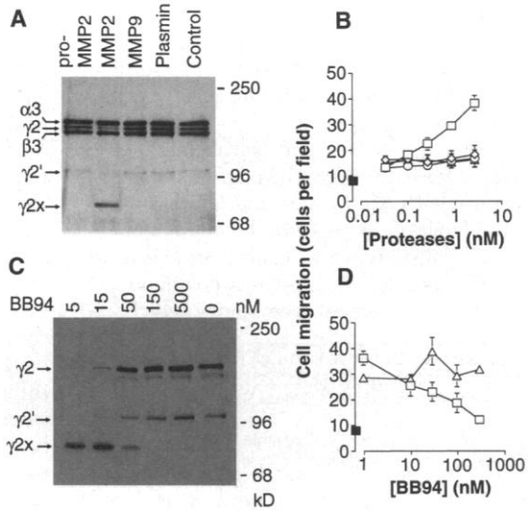

Fig. 2. Specificity of the effects of MMP2 on Ln-5. (**A**) Ln-5 is cleaved by MMP2 but not by pro-MMP2, MMP9 (*17*), or plasmin. Ln-5 (100 ng) was incubated for 2 hours at 37°C with 50 nM of the indicated proteases. Cleavage of γ2 and appearance of γ2x occurred solely in samples digested with MMP2. (**B**) MCF-10 migration on Ln-5 is induced by the addition of human activated recombinant MMP2 (□) to the medium, but not by the addition of pro-MMP2 (○), MMP9 (△), or plasmin (◇).Untreated Ln-5 (■) was used as a control. (**C**) Cleavage of the γ2 subunit by MMP2 is blocked in a dose-dependent manner by the metalloprotease inhibitor BB94. Ln-5 was incubated with 150 nM MMP2 and the indicated concentrations of BB94. Protein immunoblotting was performed with an antiserum to γ2 raised against a fusion protein encompassing domain III of the human γ2 chain (*25*). (**D**) Induction of migration by MMP2 is inhibited (□) by adding BB94 to the MMP2 pretreatment step of Ln-5, before coating the filters (see Fig. 1B). No inhibition (△) occurs when BB94 is added to the migration medium after coating the filters with MMP2-treated Ln-5. Untreated Ln-5 (■) was used as a control.

To investigate the molecular basis of this effect, we tested whether MMP2 caused structural rearrangements in Ln-5, as assessed by electrophoresis. Like the other laminins (*3*), Ln-5 comprises three disulfide-bonded subunits: α3, β3, and γ2. When electrophoresis was performed under nonreducing conditions, the molecular mass of the MMP2-treated Ln-5 heterotrimers was lower than that of untreated controls by 50 to 100 kD (Fig. 1C). Electrophoresis under reducing conditions revealed that this reduction in mass was attributable to the loss of part of the γ2 chain (Fig. 1C), which after proteolysis had a molecular mass of ~80 kD (γ2x). In contrast, the α3 and β3 subunits remained intact (Fig. 1C).

To identify the MMP2 cleavage site on Ln-5, we isolated the 80-kD γ2x fragment from MMP2-treated Ln-5 and subjected it to microsequencing. Thirteen NH_2-terminal residues were identified with the sequence Leu-Thr-Ser-Cys-Pro-Ala-Cys-Tyr-Asn-Gln-Val-Thr, which matches the sequence starting at position 587 deduced from a rat γ2 cDNA clone (Fig. 1D). The cleavage site immediately precedes two closely spaced cysteines in domain III of the γ2 subunit (Cys-Pro-Ala-Cys), which are thought to be involved in joining the α3, β3, and γ2 laminin subunits at the center of the "cross" (Fig. 1D). This location indicates that the γ2x fragment remains attached to the heterotrimer, whereas the fragment upstream of the MMP2 cleavage site dissociates, causing the observed reduction in molecular mass (Fig. 1C).

Ln-5 was not cleaved by another metalloprotease, MMP9, or by plasmin (Fig. 2A); the latter result is remarkable because plasmin is a potent serine protease affecting a broad spectrum of ECM substrates (*1*). Accordingly, neither of these proteases had any effect on cell migration (Fig. 2B). Moreover, the inactive form of MMP2, pro-MMP2, did not cleave Ln-5 or induce cell migration (Fig. 2, A and B). A metalloprotease inhibitor, BB94 (*10*), blocked MMP2-induced cleavage of the Ln-5 γ2 subunit in a dose-dependent manner (Fig. 2C). Ln-5 treated with MMP2 in the presence of the inhibitor did not induce migration (Fig. 2D). In contrast, when BB94 was added to cells plated on Ln-5 pretreated with MMP2, the cells migrated (Fig. 2D).

We next investigated how MMP2 cleavage of Ln-5 stimulates cell motility. When both HUMEC (*2*) and MCF10 cells were plated on cleaved Ln-5, they showed a change in morphology consistent with a migratory phenotype (Fig. 3A). Cells plated on cleaved Ln-5 were round, with edges projecting filopodia and lamellipodia, and had a polarized migratory appearance (Fig. 3A, right panel, inset), whereas those plat-

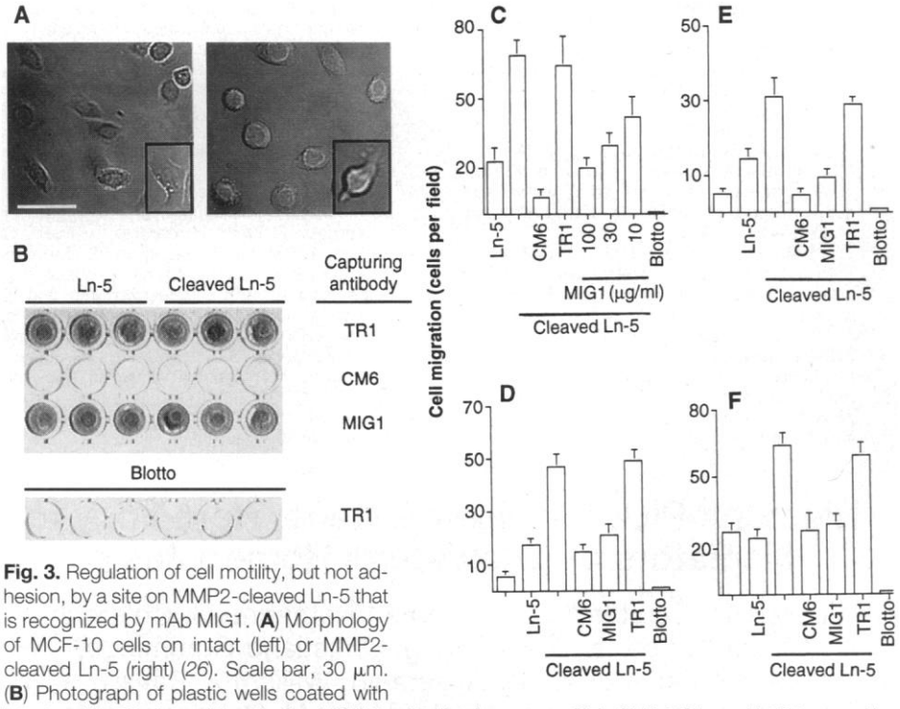

Fig. 3. Regulation of cell motility, but not adhesion, by a site on MMP2-cleaved Ln-5 that is recognized by mAb MIG1. (**A**) Morphology of MCF-10 cells on intact (left) or MMP2-cleaved Ln-5 (right) (*26*). Scale bar, 30 μm. (**B**) Photograph of plastic wells coated with intact or MMP2-cleaved Ln-5, after MCF10 cell adhesion assays (*27*). CM6, TR1, and MIG1 are mAbs reacting with distinct epitopes on the Ln-5 α3 subunit (*12*). Adhesion is about equal on intact or cleaved Ln-5, and is blocked by CM6 but not by TR1 or MIG1. In contrast (**C**), migration on MMP2-cleaved Ln-5 is blocked by MIG1 (*22*). CM6 and TR1 were used as positive and negative controls, respectively, in the migration assay. (**D** to **F**) HUMEC show no migration on basement membrane matrices Coll IV (D) and Ln-1 (E) and little migration on Fn (F). Filters were coated with Coll IV (D), Ln-1 (E), or Fn (F), and then were cocoated with the matrix indicated. In all cases, HUMEC migration is induced by co-coating the filters with MMP2-cleaved Ln-5 (*22*) but not with intact Ln-5. Induction is blocked by mAb MIG1, which is antimigratory but not antiadhesive, and by mAb CM6, which is both antimigratory and antiadhesive. Control mAb TR1 had no effect. Blotto indicates control with dry milk protein.

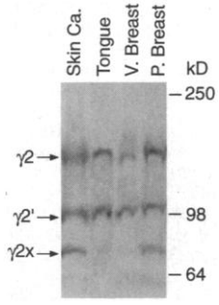

Fig. 4. Detection of 80-kD γ2 fragment (γ2x) in a rodent tumor and in tissue undergoing remodeling. Tissue extracts electrophoresed under reducing conditions were immunoblotted with antiserum to the γ2 chain (*23*). The fragment was detected in a mouse skin carcinoma (Skin Ca.) and in mammary tissue from a pregnant (13.5 days) rat (P. Breast), but not in mouse tongue or in breast tissue from a sexually immature female rat (V. Breast).

ed on uncleaved Ln-5 were large, polygonal, and often in contact with each other (Fig. 3A, left panel). Despite these morphological differences, both cell types adhered equally well to either MMP2-cleaved or uncleaved Ln-5 (Fig. 3B), and no differences were found in cell adhesion to cleaved or uncleaved Ln-5 with a centrifugal detachment assay (*7*, 9). Antibodies to integrin α3β1, a Ln-5 receptor (*11*), blocked both HUMEC and MCF10 adhesion to Ln-5 as well as migration on cleaved Ln-5 (9). These data suggest that the adhesive properties of cleaved and uncleaved Ln-5 are similar, so that changes in cell migration on MMP2-cleaved Ln-5 cannot be explained by modified adhesion strength. A monoclonal antibody (mAb) to the cell adhesion site of Ln-5 (*12*), CM6, blocked adhesion to both cleaved and uncleaved Ln-5 and, as expected, inhibited migration on cleaved Ln-5 (Fig. 3, B and C). Strikingly, mAb MIG1 (*12*), which reacts with the Ln-5 α3 subunit in protein immunoblots (9), did not block adhesion to uncleaved or cleaved Ln-5 (Fig. 3B) but efficiently blocked cell migration on cleaved Ln-5 in a dose-dependent manner (Fig. 3C).

These results indicate that the as yet unidentified MIG1 epitope on the α3 subunit represents a cryptic site on Ln-5 that is not involved in cell adhesion, yet interacts with cells and directly stimulates cell motility once it is functionally unmasked by MMP2 cleavage. Alternatively, the cleavage may mask a site that suppresses cell motility. The existence of motility-promoting cryptic sites and suppressor sites on laminins has been hypothesized, and evidence for such sites has been documented for other ECM molecules (*13*). Proteolysis of Ln-1 under nonphysiological conditions (*14*) exposes cell recognition sites that, unlike the MIG1 site, are involved in adhesion. Because the MIG1 site does not support adhesion, this epitope may have a signaling rather than a mechanical role in cell migration, which could affect the distribution, aggregation state, or turnover of integrins on the cell surface to generate proper traction for migration (*15*).

We also used various combinations of basement membrane components to examine cell motility. In the transwell migration assay, filters coated with a mixture of MMP2-cleaved Ln-5 and Coll IV, Ln-1, or Fn induced migration of both HUMEC (Fig. 3, D to F) and MCF10 cells (9). On the mixed matrices, mAb MIG1 blocked migration, which confirmed that motility was primarily induced by the cleaved Ln-5.

Finally, to explore the physiological role of this cleavage mechanism, we looked for Ln-5 heterotrimers containing the MMP2-cleaved γ2x fragment in different rodent tissues. Protein immunoblots developed with a γ2-specific antibody revealed that γ2x is present in tissues undergoing remodeling, including mammary tissue from a pregnant rat (day 13.5) and mouse carcinoma (Fig. 4). In contrast, γ2x was not detectable in control quiescent tissues, such as tongue and mammary tissue from a sexually immature female rat (Fig. 4).

Our results demonstrate that Ln-5 is a primary target of MMP2 enzymatic cleavage and is critical for cell migration during tissue remodeling and tumor invasion. In addition, they indicate that MMP2, whose functional importance was thought to be limited to the physical destruction of ECM barriers (*1*), provides a signaling mechanism for cells to begin migration. MMP2 is expressed in stromal cells surrounding tumor buds (*1*), and Ln-5 is expressed in breast and colon cancer cells at their invasive edge (*6*). These findings and our results highlight the potential importance of these two molecules in the development and spread of cancer. Future treatments designed to block MMP2 cleavage of Ln-5 may provide new tools to combat cancer cell invasion.

REFERENCES AND NOTES

1. H. Birkedal-Hansen, *Curr. Opin. Cell Biol.* **7**, 728 (1995); J. Gailit and R. A. Clark, *ibid.* **6**, 717 (1994); W. T. Chen, *ibid.* **4**, 802 (1992); E. C. Kohn and L. A. Liotta, *Cancer Res.* **55**, 1856 (1995).

2. P. C. Brooks *et al.*, *Cell* **85**, 683 (1996); H. Sato *et al.*, *Nature* **370**, 61 (1994); C. B. Basbaum and Z. Werb, *Curr. Opin. Cell Biol.* **8**, 731 (1996).
3. R. E. Burgeson *et al.*, *Matrix Biol.* **14**, 209 (1994); G. W. Laurie, C. P. Leblond, G. R. Martin, *J. Cell Biol.* **95**, 340 (1982).
4. S. E. Baker *et al.*, *J. Cell Sci.* **109**, 2509 (1996).
5. K. Miyazaki, Y. Kikkawa, A. Nakamura, H. Yasumitsu, M. Umeda, *Proc. Natl. Acad. Sci. U.S.A.* **90**, 11767 (1993).
6. P. Basset *et al.*, *Nature* **348**, 699 (1990); C. Monteagudo, M. J. Merino, J. San-Juan, L. A. Liotta, W. G. Stetler-Stevenson, *Am. J. Pathol.* **136**, 585 (1990).
7. A. J. Pelletier, T. Kunicki, V. Quaranta, *J. Biol. Chem.* **271**, 1364 (1996).
8. H. D. Soule *et al.*, *Cancer Res.* **50**, 6075 (1990).
9. G. Giannelli and V. Quaranta, unpublished data.
10. X. Wang, X. Fu, P. D. Brown, M. J. Crimmin, R. M. Hoffman, *Cancer Res.* **54**, 4726 (1994).
11. M. Hormia *et al.*, *J. Invest. Dermatol.* **105**, 557 (1995).
12. G. Plopper *et al.*, *J. Cell Sci.* **109**, 1965 (1996).
13. A. L. Calof, M. R. Campanero, J. J. O'Rear, P. D. Yurchenco, A. D. Lander, *Neuron* **13**, 117 (1994); S. Stefansson and D. A. Lawrence, *Nature* **383**, 441 (1996).
14. M. Aumailley, M. Gerl, A. Sonnenberg, R. Deutzmann, R. Timpl, *FEBS Lett.* **262**, 82 (1990); P. I. Karecla, R. Timpl, F. M. Watt, *Cell Adhes. Commun.* **2**, 309 (1994).
15. D. A. Lauffenburger and A. F. Horwitz, *Cell* **84**, 359 (1996).
16. Y. Itoh, S. Binner, H. Nagase, *Biochem. J.* **308**, 645 (1995).
17. S. M. Wilhelm *et al.*, *J. Biol. Chem.* **264**, 17213 (1989).
18. G. Giannelli *et al.*, *Lab. Invest.* **74**, 1091 (1996).
19. M. Langhofer, S. B. Hopkinson, J. C. R. Jones, *J. Cell Sci.* **105**, 753 (1993).
20. C. A. Burdsal, M. C. Alliegro, D. R. McClay, *Dev. Biol.* **144**, 327 (1991).
21. R. Fridman *et al.*, *Biochem. J.* **289**, 411 (1993).
22. For migration assays (*7*), transwell filters were coated on the underside with Ln-5 (1 μg/ml), Coll IV (10 μg/ml, Gibco-BRL), Ln-1 (20 μg/ml; Collaborative, Becton-Dickinson, Bedford, MA), or Fn (20 μg/ml, Gibco-BRL). Filters were washed and cells were plated in the upper transwell chamber. After 16 hours at 37°C, filters were fixed and stained, and cells that migrated to the underside were quantified by counting four microscopic fields from duplicate filters. Results are the mean number of cells counted in each field ± SD. In some experiments (Fig. 3C), after blocking, filters were incubated with indicated mAbs (100 μg) (*12*). In Fig. 3, D to F, filters precoated with Ln-1, Coll IV, or Fn were recoated with MMP2-cleaved Ln-5 followed by addition of BB94 and mAbs.
23. Rat Ln-5 was purified from the spent media of 804G cells (*11*). As judged by SDS–polyacrylamide gel electrophoresis (PAGE), some Ln-5 purified preparations contain a small amount of γ2 that migrates as a band at 135 kD. Ln-5 (100 ng) was incubated for 2 to 24 hours at 37°C with indicated concentrations of recombinant activated MMP2 (*16*), inactive pro-MMP2, recombinant active MMP9 (*17*), or highly purified plasmin (Enzyme Research Laboratory, South Bend, IN), and then analyzed by protein immunoblotting (*18*). The same results were obtained with semipurified Ln-5 (*9*). We verified activation and purity of MMP2 and MMP9 by zymography (*18*). We determined that plasmin cleaved fibrinogen with the expected pattern even at concentrations 1000 times the Ln-5 concentration used. Polyclonal antiserum 2163 to the γ2 chain was from rabbits injected with γ2′ protein, purified by excision from SDS-PAGE gels (*19*). Tissues were pulverized, resuspended in 0.05 M tris-HCl (pH 7.4), 0.01 M EDTA, BB94 (50 ng/ml), and phenylmethylsulfonyl fluoride (1 mg/ml), and centrifuged at 17,200*g* for 30 min at 4°C; the pellet was resuspended in sample buffer, sonicated, and analyzed by protein immunoblot. Cleaved Ln-5 was prepared as described (*18*), and the NH_2-terminal sequence from the 80-kD polypeptide was obtained by automated Edman degradation. Rat γ2 cDNA was cloned by homology screening and sequenced from an 804G cell λgt11 cDNA library (Clontech, Palo Alto, CA).
24. M. P. Marinkovich, G. P. Lunstrum, R. E. Burgeson, *J. Biol. Chem.* **267**, 17900 (1992).
25. C. Pyke *et al.*, *Cancer Res.* **55**, 4132 (1995).
26. MCF-10 cells were plated for 2 hours at 37°C on glass cover slips coated with Ln-5 (*19*), washed, fixed, and photographed with an Axiovert 135 microscope (Zeiss).
27. The mAbs TR1, CM6, and MIG1 (20 μg/ml) were adsorbed for 1 hour at room temperature on 96-well plates (Sarstedt, Sparks, NV). After blocking, intact or cleaved Ln-5 was captured in wells for 2 hours, and 8×10^4 cells per well were added in Dulbecco's modified Eagle's medium with 1% bovine serum albumin. Plates were incubated at 37°C in a humidified incubator under 10% CO_2 for 30 min, filled with phosphate-buffered saline (PBS), inverted, and gently shaken in a tank of PBS for 15 min. Excess PBS was removed, and adherent cells were fixed, stained with crystal violet, solubilized, and quantified by densitometry (*11*). To measure strength of adhesion, we performed a detachment assay (*20*). Radiolabeled cells were incubated on matrix-coated polystyrene plates and were detached by inverted centrifugation for 8 min at 80, 1200, 1450, or 1700*g*; the remaining cells were quantified on a Molecular Dynamics PhosphorImager.
28. We thank British Bio-Technology Ltd. for BB94, Desmos Inc. for purified Ln-5, and K. Tryggvason for antisera; Z. Werb, H. Gardner, A. Pozzi, G. Plopper, A. Pelletier, F. Frasier, and S. Carter for technical support, assistance, and discussions; L. Bibbs for help with microsequencing; and Z. Ruggeri for help with microscopy. Supported by NIH grants DE10063 and CA47858 (V.Q.), an Istituto Superiore di Sanità fellowship (G.G.), and a Deutsche Forschungsgemeinschaft fellowship (J.F.-M.).

3 December 1996; accepted 3 June 1997

Niemann-Pick C1 Disease Gene: Homology to Mediators of Cholesterol Homeostasis

Eugene D. Carstea,* Jill A. Morris,* Katherine G. Coleman, Stacie K. Loftus, Dana Zhang, Christiano Cummings, Jessie Gu, Melissa A. Rosenfeld, William J. Pavan, David B. Krizman, James Nagle, Mihail H. Polymeropoulos, Stephen L. Sturley, Yiannis A. Ioannou, Maureen E. Higgins, Marcella Comly, Adele Cooney, Anthony Brown, Christine R. Kaneski, E. Joan Blanchette-Mackie, Nancy K. Dwyer, Edward B. Neufeld, Ta-Yuan Chang, Laura Liscum, Jerome F. Strauss III, Kousaku Ohno, Marsha Zeigler, Rivka Carmi, Jacob Sokol, David Markie, Raymond R. O'Neill, O. P. van Diggelen, Milan Elleder, Marc C. Patterson, Roscoe O. Brady, Marie T. Vanier, Peter G. Pentchev,† Danilo A. Tagle

Niemann-Pick type C (NP-C) disease, a fatal neurovisceral disorder, is characterized by lysosomal accumulation of low density lipoprotein (LDL)–derived cholesterol. By positional cloning methods, a gene (*NPC1*) with insertion, deletion, and missense mutations has been identified in NP-C patients. Transfection of NP-C fibroblasts with wild-type *NPC1* cDNA resulted in correction of their excessive lysosomal storage of LDL cholesterol, thereby defining the critical role of NPC1 in regulation of intracellular cholesterol trafficking. The 1278–amino acid NPC1 protein has sequence similarity to the morphogen receptor PATCHED and the putative sterol-sensing regions of SREBP cleavage-activating protein (SCAP) and 3-hydroxy-3-methyl-glutaryl coenzyme A (HMG-CoA) reductase.

Genetic disorders have helped to define critical steps of cellular metabolism. For example, elucidation of the biochemical and genetic defects underlying familial hypercholesterolemia (FH) laid the cornerstone for the discovery of the LDL-receptor pathway of cellular cholesterol metabolism (*1*). Similarly, the role of lysosomes and cholesteryl ester (CE) hydrolase in the processing of the CE core of LDL was revealed by Wolman's syndrome, a lysosomal CE storage disease (*2*).

Niemann-Pick type C (NP-C) disease is an inherited lipid storage disorder that affects the viscera and central nervous system (*3*). It occurs at low frequency (affecting one in 10^6 individuals) and is inherited in an autosomal recessive manner. Both linkage and complementation analyses have shown that at least two separate genes, *NPC1* (major locus) and *NPC2*, induce identical clinical and biochemical phenotypes (*4*). Cells from NP-C patients are defective in the release